Journal of Membrane Science 596 (2020) 117691

Contents lists available at ScienceDirect

Journal of Membrane Science

journal homepage: http://www.elsevier.com/locate/memsci

NMR diffusion studies of proton-exchange membranes in wide temperature range

Elena Galitskaya [a], Alexei F. Privalov [b], Max Weigler [b], Michael Vogel [b], Alexei Kashin [c], Mikhail Ryzhkin [a], Vitaly Sinitsyn [a,*]

[a] Institute of Solid State Physics RAS, 2 Academician Ossipyan str, 142432, Chernogolovka, Russia
[b] Institute für Festkorperphysik, Technische Universitat Darmstadt, Hochschulstr. 6, 64289, Darmstadt, Germany
[c] Inenergy LLC, Electrodnaya str., 12-1, 111524, Moscow, Russia

ARTICLE INFO

Keywords:
Proton-exchange membrane (PEM)
NMR diffusometry
Low temperature diffusion in PEM
Ice rules
Proton transport mechanism

ABSTRACT

The diffusion coefficients in proton-exchange perfluorosulfonated membranes fabricated by different techniques have been analyzed in the temperature range from 200 K to 300 K using NMR diffusometry in a static magnetic gradient field. The influence of the water content as well as the effects of the membrane thickness and the side-chain length on the diffusion coefficient was analyzed. It is found that the fabrication by the extrusion cast method leads to faster diffusion as compared to the solution cast fabrication method. Shorter side chains are also preferable for faster diffusion. Both the decrease of the temperature and the water content leads to a reduced diffusion coefficient, affecting the transport micromechanism in a similar way by increasing the role of the water on the pore walls with respect to proton transport. The model of confined water in Nafion pores has been applied to analyze the results. It is proposed that both conductivity and diffusion at low temperatures are determined by protonic transport of the surface water via bond defects in contrast to the bulk water or ice, where the ionic defects are responsible for the mass transport.

1. Introduction

The most developed technology for direct conversion of chemical energy to electric energy without combustion involves proton-exchange membrane fuel cells (PEMFCs) [1–4]. PEMFCs operate in the following way: an oxidizer (usually air) is supplied on an electrochemical cell from the cathode side and fuel (usually hydrogen) is fed from the anode side. A chemical reaction at the anode produces proton–electron pairs. The electrons are sent to a load, while the protons migrate through the membrane, thereby reacting in the cathode region with oxygen to water. Electrolytic membranes currently used in PEMFCs are perfluorosulfonated polymers such as Nafion, where the proton transport occurs via water confined in nanochannels. In this case, the migration of protons through the membrane is accompanied by electroosmosis: the moving protons entrain the neutral water molecules from anode to cathode. It was established that in this type of polymers each proton picks up about three water molecules [5,6]. As a result, a deficit and an excess of water arise in the anode and the cathode regions, respectively, causing a concentration gradient and, therefore, an inverse diffusion flow of H_2O molecules. Thus, the processes of diffusion play a significant role in the operation of PEMFCs and it is important to study how it depends on the water content and the temperature. The temperature range must be wide, taking into account the practical applications in various climatic conditions.

2. Studies of water diffusion in sulfonated polymer membranes

Water diffusion in perfluorosulfonated membranes was intensively studied in the past [7–17]. These studies were performed primarily on commercial Nafion 117 membranes obtained by the extrusion cast method. The water content in Nafion 117 membranes is usually related to the equivalent weight of sulfite groups in the polymer: $\lambda = N_{H2O}/N_{SO3H}$ at room temperature. It was found that the diffusion coefficient increases rapidly with increasing water content if λ is below ~3–4 whereas the diffusion coefficients dependence from the amount of water became more flatten at $\lambda > 5$ [7–17] and this behavior safe at sub-freezing temperatures [18]. A similar dependence of the diffusion coefficient on λ was also observed for other types of membranes, while

* Corresponding author.
E-mail address: sinitsyn@issp.ac.ru (V. Sinitsyn).

https://doi.org/10.1016/j.memsci.2019.117691
Received 6 August 2019; Received in revised form 26 November 2019; Accepted 27 November 2019
Available online 29 November 2019

the values of the diffusion coefficients can differ significantly for samples, which have the same nominal composition [7,8,13].

Such discrepancies could result from different conditions of membrane preparations, irreproducible saturation with water, etc. In particular, inconsistent diffusion coefficients were obtained for extrusion Nafion 117 and Nafion 112 membranes at low temperatures [10, 12]. The authors of [10] detected a stepwise decrease in the self-diffusion coefficient of water in the Nafion 117 membrane at ~253 K. At the same time, the self-diffusion coefficient measured for the Nafion 112 membrane varies smoothly with temperature, showing only a small change in the slope [12]. Authors [18] also did not observed any stepwise anomalies in diffusion coefficients of Nafion 117 membrane measured at 98% humidity but they did not present λ data, which do not allow us to directly compare with ref's 10 and 12. It is noteworthy that the Nafion 117 and the Nafion 112 membranes are distinguished by their thickness. Thus, it is still interesting also to determine the influence of the membrane thickness on the diffusion coefficient and its temperature dependence at close water contents.

A very important structural feature of perfluorosulfonated polymers is the presence of a system of pores connected by nanochannels, through which the diffusion of water molecules and proton transport occurs [19–21]. The state of confined water is significantly different from the state of bulk water. In particular, water in perfluorosulfonated polymer membranes can be in a free state with the characteristics corresponding to bulk water, in a state strongly coupled to sulfonic acid groups with lower dielectric relaxation frequencies, and in a weakly coupled state with higher dielectric relaxation frequencies [22–25].

The model for the water behavior in nanochannels of porous materials, in particular in proton-exchange membranes, has been presented in ref's [22,23], where were suggested that the water in nanochannels exist in two different states. The first state is bulk water in the center of the pores with usual characteristics. The second state is the surface water with an abundance of hydrogen bonds in the wall vicinity and strong violations of the ice rules [26]. Similar behaviors are known for water in various types of confinements [27–31].

The application of NMR to study the diffusion coefficients of H_2O in Nafion has a long tradition, starting almost three decades ago [7]. Nowadays NMR diffusometry is an established method and we will apply it to proton-exchange membranes. Specially, the ^1H diffusion coefficients in various membranes are measured using an ultrahigh static gradient magnetic field (SFG NMR) in the temperature range from 200K to 300 K. The studies are performed on membranes obtained from Chemours (Nafion membranes), fabricated by extrusion cast and solution cast methods and from Fumatech (Fumapem membranes) with different lengths of the side chains but the same equivalent weights fabricated by the solution cast method. The goal of this work is to compare diffusion coefficients in proton-exchange membranes fabricated by different methods, differing also by their thicknesses and side-chain lengths in a wide temperature range. Another goal is to show that the model [21] enables an explanation of the experimental data.

3. Experimental

3.1. Sample preparation

The commercial membranes were first pretreated by cleaning. The samples were boiled in 3 wt % hydrogen peroxide solution (H_2O_2) during 1 h and rinsed with distilled water to eliminate organic impurities. To remove residual hydrogen peroxide, the membranes were boiled in distilled water for 1 h. The final protonation procedure included exposition of the samples to 0.5 M sulfuric acid (H_2SO_4) for 1 h and followed by boiling in distilled water for 1 h in accordance with [7]. The cleaned membranes were cut into 1 cm × 5 cm stripes. To erase memory effects, the membranes were annealed at 80 °C in a vacuum under 0.1 bar for 20 h and were kept at $T = 25$ °C under 0.1 bar for 20 h. Finally, the samples were dried at 25 °C under 5×10^{-6} mbar for 48 h.

In order to obtain the desired water content in the samples, the membrane stripes were placed in a desiccator containing a saturated solution of the proper salt to control the humidity ($MgCl_2$-33%RH, $KBrO_3$-98%RH). The desiccators were darkened and kept at a temperature of 23 °C. The weight of the samples was stable after 14 days of wetting. Afterwards the samples were inserted into the NMR tubes, which were closed by teflon caps. In order to avoid a humidity loss, the caps were sealed with a small amount of epoxy resin. The samples were weighed at the beginning and at the end of the experiment to ensure the absence of water loss.

3.2. NMR diffusometry

In order to quantify the influence of the sample characteristics on the dynamic properties, the self-diffusion coefficients of protons were measured using ^1H Static Field Gradient (SFG) NMR diffusometry [32, 33]. The SFG method has high gradient of magnetic field and allows to measure the systems with short T_1 and T_2 relaxation times, since SFG does not require gradient switching. For these measurements a three pulse stimulated echo sequence was used which provides an echo amplitude S, the decay of which is mainly governed by spin relaxation and diffusion:

$$S(t_p, t_m, g) = S_0 \cdot \exp\left(\frac{-t_m}{T_1}\right) \cdot \exp\left(\frac{-2t_p}{T_2}\right) \cdot \exp\left[-(\gamma g t_p)^2 \cdot \left(\frac{2}{3}t_p + t_m\right) \cdot D \right] \quad (1)$$

While t_p is the interval between the first two RF pulses of the stimulated-echo sequence and t_m is the interval between the second and the third pulses in this sequence, T_1 and T_2 are the spin-lattice and spin-spin relaxation times respectively, γ is the ^1H gyromagnetic ratio, g is the field gradient and D is the diffusion coefficient. To independently determine the decays due to spin relaxation, we performed a separate experiment in a homogeneous field at the same frequency and temperatures. The T_1 and T_2 times were measured using standard NMR techniques and all measured T_1 dependencies have shown mono-exponential behaviour. The T_2 filtering method was applied to cut off the contribution to the NMR signal from the ice phase. Typical diffusion lengths during experiments were in the rage from hundreds of nm to tens of μm. The static field gradient was generated by a specially constructed magnet with anti-Helmholtz arrangement of superconducting coils, yielding a maximum field gradient of 180 T/m [32,34,35]. The ^1H NMR frequency in our experiment was 162 MHz, the field gradient was 141 T/m and the length of 90-degree RF pulses was 0.7μs. The measurements were carried out in a temperature range from 200 to 300 K. The temperature was set with an accuracy of 1 K and stabilized to 0.1 K. The diffusion coefficient errors were calculated at fitting echo signals. The major uncertainty in NMR diffusion coefficient arising from the determination of the magnetic field gradient, which is below 1% and from the unavoidable experimental noise of the measured echo amplitude $S(t_p,t_m, g)$, affecting the fitting with Eq. (1). Experimental noise is controlled by the number of accumulations to get the final accuracy usually better than 3%. At temperatures below 250K the diffusion becomes slower while the T_1 and the T_2 relaxation times becomes shorter. The proper exponents with relaxation terms in Eq. (1) get dominating over the exponent with diffusion coefficient, which leads to a gradual decrease in accuracy to 10%.

4. Results

4.1. Influence of membrane thickness and fabrication method

Fig. 1 shows the Arrhenius plot of the diffusion coefficients D for Nafion 211, 212 and 117 membranes at a high water content (wetted at 98% RH, λ ≈ 6–7). Nafion 211 and 212 were obtained by the solution cast method and have thicknesses d of 25 and 50 μm, respectively. Their

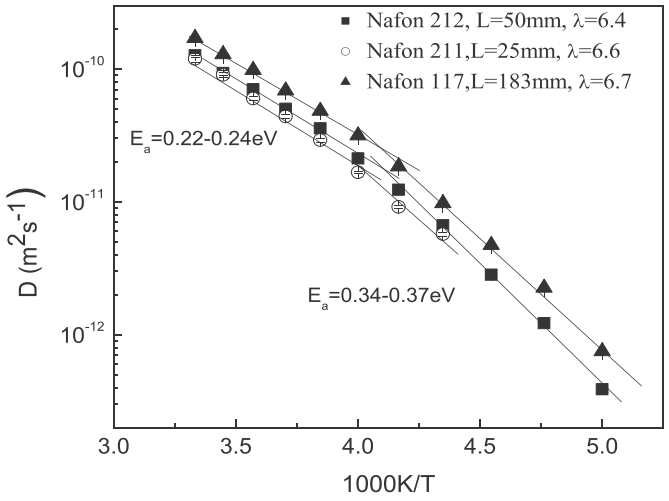

Fig. 1. Temperature dependent self-diffusion coefficients for the Nafion 211, Nafion 212 (solution cast method) and Nafion 117 (extrusion cast method) membranes at high water content λ.

self-diffusion coefficients are nearly the same indicating that proton transport does not depend on sample thickness. For the Nafion 117 membrane (d = 180 μm) obtained by extrusion, the self-diffusion coefficient is, within the entire temperature range, about 1.5 times higher than for the solution cast membranes. Thus, the difference in thickness hardly affects the diffusion, while the fabrication method does.

The *D*(T) dependencies for all investigated samples reveal two temperature intervals where they obey to the Arrhenius law:

$$D(T) = D_0 \cdot \exp\left(\frac{-E_a}{kT}\right). \quad (2)$$

where D_0 is the pre-exponential factor, E_a is the activation energy, T is the temperature, *k* is Boltzmann constant. For all samples the diffusion coefficients demonstrate a change in slope (knee) at around $T = 240$ K. This corresponds to two different regimes with activation energies E_a of ~0.20 eV above 240 K and 0.35–0.43 eV below 240 K. However, the transition between the two regimes is smooth. The activation energies E_a for all samples are collected in Table 1.

It should be noted that the knee on *D*(T) dependences is close to the value of the singularity temperature for confined water in Nafion determined in Ref. [36]. The nature of this singularity in bulk water has been the subject of some discussion [37–39]. The authors [36] suggested that at this temperature the orientation motion of water molecules is frozen. Therefore, the observed increase in the activation energy of the diffusion coefficients at T < 240K indicates a change in the diffusion micromechanism, which is discussed below.

4.2. Influence of side chain length and water content

Effects of the side chain length are studied using Fumapem F950 membrane with long side chains and Fumapem FS 930 RFS membrane with short side chains. The chemical structure of the perfluorite sulfonated polymers with different side chains are described in detail in Refs. [40,41]. Both membranes were obtained by the solution cast method and have identical equivalent weight ≈950 g/eq. In this way it is possible to almost exclude an influence of SO_3^{2-} group concentration on the diffusion coefficient and to obtain samples with water contents close to each other after saturation in an atmosphere with a fixed humidity. In addition, we analyze the role of the water content by preparing these samples with high (λ ≈ 8) and low (λ ≈ 2) amounts of water. The temperature-dependence of *D* values of these samples are presented in Fig. 2.

We see that the temperature dependences of D_{NMR} for λ ≈ 8 for both

Table 1
The values of activation energy E_a and pre-exponential factor D_0 for measured membranes. The errors of E_a and D_0 parameters were determined at fitting experimental data with Eq. (2)

N°	sample	d, μm	EW, g/eq	λ	temperature interval, K	D_0, m^2/s	E_a, eV
1	Nafion 117	183	1100	2.6	200–240	(1.25 ± 0.01) E−2	0.46 ± 0.01
2	Nafion 212	50	1100	6.4	200–240	(9.74 ± 0.03) E−4	0.37 ± 0.01
3	Nafion 211	25	1100	6.6	200–240	–	~0.35
4	Nafion 117	183	1100	6.7	200–240	(2.29 ± 0.03) E−4	0.34 ± 0.01
5	F 950	50	950	8.3	200–240	(1.94 ± 0.01) E−2	0.42 ± 0.01
6	FS 930 RFS	30	930	8.6	200–240	(1.78 ± 0.02) E−3	0.37 ± 0.01
7	FS 930 RFS	30	930	1.4	250–300	(8.8 ± 0.1)E−6	0.31 ± 0.01
8	F 950	50	950	1.5	250–300	(7.7 ± 0.1)E−6	0.32 ± 0.01
9	Nafion 117	183	1100	2.6	250–300	(1.1 ± 0.1)E−6	0.25 ± 0.01
10	Nafion 212	50	1100	6.4	250–300	(8.0 ± 0.1)E−7	0.23 ± 0.01
11	Nafion 211	25	1100	6.6	250–300	(1.20 ± 0.1)E−6	0.24 ± 0.01
12	Nafion 117	183	1100	6.7	250–300	(7.8 ± 0.1)E−7	0.22 ± 0.01
13	F 950	50	950	8.3	250–300	(4.7 ± 0.1)E−7	0.20 ± 0.01
14	FS 930 RFS	30	930	8.6	250–300	(1.4 ± 0.1)E−6	0.22 ± 0.01

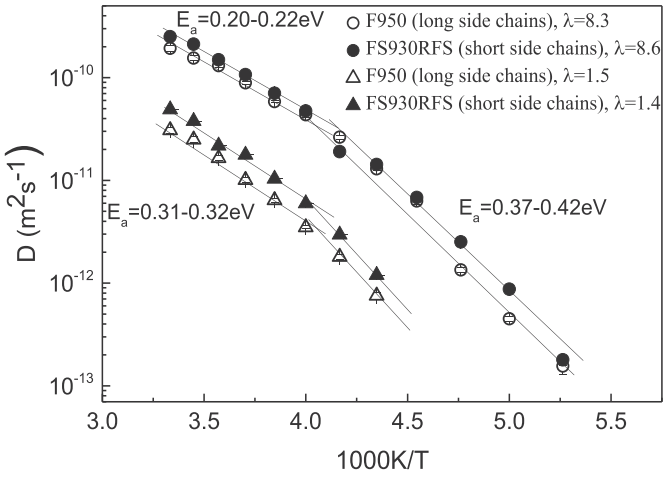

Fig. 2. Temperature-dependent self-diffusion coefficients for Fumapem F950 membrane with long side chains and for FS930 RFS membrane with short side chains at high and low water contents λ.

membranes are almost identical. The D_{NMR} values for these membranes at high water contents appear somewhat higher than those for the Nafion membranes at the same temperatures, see Fig. 2. However, the activation energies E_a = 0.20–0.22 eV and 0.37–0.42 eV above and below ~240 K, respectively almost coincide with the activation energies for the Nafion membranes. The self-diffusion coefficients at low water contents are about an order of magnitude lower over the whole temperature range, while the temperature dependences of D_{NMR} repeat the

behavior measured for the samples with a high water content and can be described by nearly the same activation energies (Fig. 2).

Thus, the diffusion mechanism in Fumapem membranes changes near $T = 240$ K and this change is independent of the concentration of sulfite groups, from the length of the side chains and also from the diameter of the channels which is weakly dependent from λ. We also would like to note that the self-diffusion coefficient for the membrane with short side chains at low water content, $\lambda \approx 2$, is somewhat higher than for the membrane with long side chains. Thus the short-chain membranes have advantages for fuel cells while operating at low humidity.

4.3. Comparison of NMR and conductivity results

There are several works presented behavior of protonic conductivity in Nafion below water melting point [42,43,46] and proposed empirical expression describing protonic conductivity in wide temperature and water content ranges. However, more detail conductivity measurements with precise water content determination for cooling and heating processes were carried out in Ref. [44]. It can be seen from Fig. 3 that the self-diffusion coefficient and the total conductivity [44] behave similarly if the water content is high ($\lambda \geq 6$), their activation energies are close to each other and the conductivity temperature dependence also exhibits a transition from high to low activation energy approximately at the same temperature of 240 K. The activation energy is about 0.2 eV at high water content in the high-temperature region, which is close to 0.16 eV of the high-frequency conductivity of bulk water [45].

At low water content ($\lambda \approx 2$–3), the used methods yield different results for the temperature dependence. At temperatures below 240 K the activation energy of the electroconductivity amounts to 0.56 eV, while NMR diffusometry gives only 0.46 eV. In the high-temperature region these values are 0.34 eV and 0.25 eV respectively (Fig. 3). This difference probably suggests a change in the conduction mechanism when the water content λ is reduced to values below 3.

Therefore, we conclude that the decrease of water content and temperature reduce the proton mobility in Nafion membranes. The mechanisms for diffusion and conductivity change at around 240 K, (will be discussed below) affecting the activation energy. Furthermore, conductivity and diffusivity show similar behavior at high water content, whereas the mechanism for charge transport deviates from that for diffusion at low water content of $\lambda \approx 3$. The similar temperature and water contents effects on transport properties in Nafion were remarked in recent review [46]. The authors [46] concluded that the complex nature of conductivity involving water-mediated transport, proton hopping, and segmental motion of chains, all contribute to the thermally activated kinetics of proton mobility that changes significantly with water content. However, no any microscopic description model of transport properties in Nafion was proposed.

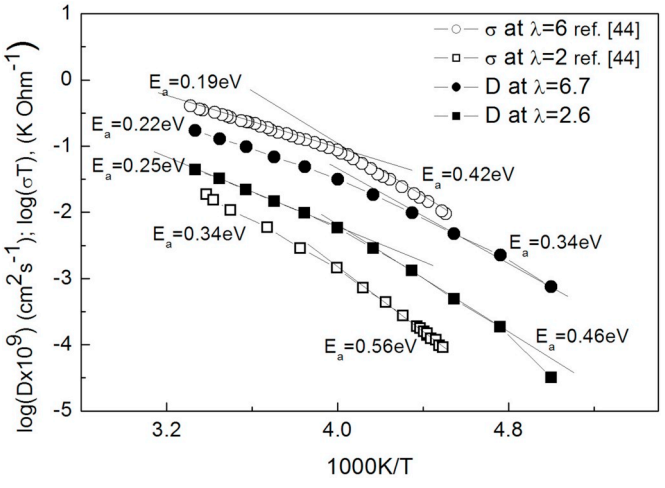

Fig. 3. Temperature dependences of the proton self-diffusion coefficient and proton conductivity for the Nafion 117 membrane at similar water contents λ. The conductivity data are taken from Ref. [44].

5. Model of confined water

For the interpretation of our results we describe water confined to the nanochannels of the Nafion polymer films by a model which is based on the theory of proton transport in ice [47–53]. The ice rules mean, that the protons are distributed over all possible positions on hydrogen bonds as: two protons near each oxygen ion and one proton on each hydrogen bond [47–53]. The proton transport is prohibited in the system and could be realized only via ionic and bond defects. The idea of present description is that the structural properties of water at the membrane walls are similar to that of ice where different defects resulting from violations of the ice rules are possible. The Coulomb interaction between such defects leads to a temperature-induced increase of their concentrations by 6–7 orders of magnitude [51]. This can be treated as a first order phase transition, which is accompanied by a commensurate decrease in the relaxation time and can be interpreted as the formation of a liquid like state of dynamically disordered hydrogen bonds. The approach is based on the Jaccard theory [26,47–53] initially developed for electric properties of ice. According to this theory, the electric properties of ice can be described in terms of proton point defects H_3O^+, OH^-, D, and L, which stem from the violations of ice rules as shown in Fig. 4. The process formation of two ionic defects H_3O^+ and OH- involve at the beginning the proton jump along the hydrogen bond when a pair of charged defects (H_3O^+ and OH^-) is at the minimum possible distance. Then ionic defects migrate on some distance by the subsequent jumps of protons along the hydrogen bonds network, as shown by arrows on Fig. 4. It is important to note that ionic defects are always born in pairs, and that they are always connected by a string of equally ordered hydrogen bonds, shown in this figure by arrows. Fig. 4b shows the formation process of a pair of bond defects (L and D), that is, hydrogen bonds with two (L) and zero (D) protons which accompanying by broken of H-bond. These defects are called bond defects, or orientation defects. As can be seen from Fig. 4b, they are also born in pairs, carry an electric charge, and are also connected by a string of equally oriented hydrogen bonds along the separation path.

To provide a compact description of the charge transport we will turn from the description of the electric processes in terms of strongly interacting molecules to a quasi-particle representation with weak interactions among excitations (the defects).

The main equations of the Jaccard theory are [26,47,53]:

$$\frac{\partial \mathbf{\Omega}}{\partial} = \sum_{k=1}^{4} n_k \mathbf{j}_k \tag{3}$$

$$\mathbf{j}_k = \frac{\sigma_k}{e_k^2}[e_k \mathbf{E} - \eta_k \Phi \mathbf{\Omega}] \tag{4}$$

Equation (3) describes the time evolution of the vector $\mathbf{\Omega}$ characterizing the ordering (or polarization) of hydrogen bonds, which is related to the arrangement of defects, as shown in Fig. 4. Eqs. (3) and (4) are the equations of linear response theory to describe the fluxes induced by the electric field $\mathbf{E}$ and the configuration vector $\mathbf{\Omega}$. In Eq. (4), the subscripts $k = 1,\ 2,\ 3,$ and 4 specify H_3O^+, OH^-, D, and L defects respectively; $\eta_k = +1, -1, -1, +1$ are the coefficients characterizing the way of polarization of hydrogen bonds (see Fig. 4); and $\mathbf{j}_k$ is the defect flux density. In Eq. (4), e_k *and* σ_k are the effective charges and partial conductivities of defects, respectively, $\Phi = 8kTr_{00}/\sqrt{3}$ specifies the entropy force acting on a defect and it is calculated in Ref. [38], The coefficient Tr_{oo} defines a generalized thermodynamic force, also called a configuration or entropy force, on the side of the configuration vector. The configuration vector characterizes the order of the proton subsystem

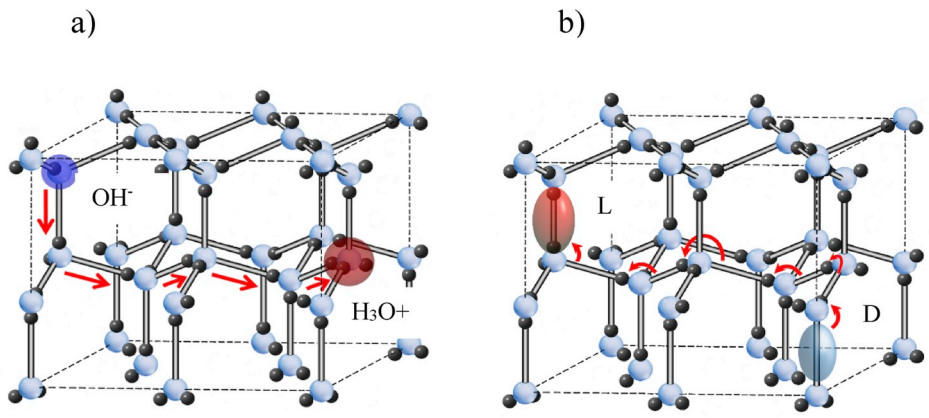

Fig. 4. Formation and motion of H_3O^+,OH^- (a), D, L– defects (b): oxygen ions bound to three and one proton, and bonds with two and zero protons respectively. Defects are indicated by corresponding ovals. Proton hopping leads to a displacement of defects and a polarization of the bonds over the covered distances.

resulting from the defects motions; T is the temperature and r_{OO} is the distance between the nearest oxygen ions.

Equations (3) and (4) lead to a Debye type frequency dependent conductivity, which can be written in the form

$$\sigma(\omega) = \sigma_1 + \sigma_2 + \sigma_3 + \sigma_4 - \frac{\Phi\tau[(\sigma_1+\sigma_2)/e_1 - (\sigma_3+\sigma_4)/e_3]^2}{1 - i\omega\tau} \quad (5)$$

$$\tau^{-1} = \Phi\left[(\sigma_1+\sigma_2)/e_1^2 + (\sigma_3+\sigma_4)/e_3^2\right] \quad (6)$$

where τ is the Debye relaxation time. In ordinary ice the conductivity due to ionic defects must be equal to the conductivity due to bond defects and the relation $\sigma_1+\sigma_2 = \sigma_3+\sigma_4$ is satisfied in the static and high-frequency conductivities and can be expressed in the form [26,47,48]:

$$\sigma(0) = \frac{e^2}{e_1^2}(\sigma_1+\sigma_2), \quad \sigma(\infty) = \sigma_3+\sigma_4, \quad \tau^{-1} = \frac{\Phi}{e_3^2}(\sigma_3+\sigma_4) \quad (7)$$

The dc or low frequency conductivity is determined by minority carriers, which are slow, whereas the high-frequency conductivity and relaxation times are determined by the fast majority carriers.

We emphasize that Eq. (7) is obtained for partial conductivities and in the general case Eqs. (5) and (6) should be used. The physical meaning is the following: if an electric field is applied, the majority carriers carry the main current and polarize the bonds. This stops the current of the majority carriers (see Fig. 4) and in this polarized state only a weak current of minority carriers is possible. Thus, in the ice the polarization and the conductivity are present.

With increasing temperatures, the proton subsystem in ice can undergo a phase transition to a new state where the defect density is many orders of magnitude higher than the carrier density [50–52]. In this case, the relative concentration of bond defects, which are in fact broken hydrogen bonds, reaches about 10% immediately after the transition. The sharp increase of concentration of broken hydrogen bonds results in a sharp increase of the number of the oxygen vacancies and their mobility. According to the Frenkel vacancy theory of melting, the last property allows one to treat this new state as a liquid state. Thus, we can interpret the water as ice with strongly broken hydrogen bonds. This is an extremely radical treatment of water, but nevertheless it allows to interpret the transport properties of water in a very accurate agreement with experiments [10,50,51], where the properties of water confined in nanochannels have been found fundamentally different from the properties of bulk water. According to the modern treatment, the water holds more than 90% of hydrogen bonds, which allows to describe such water with retained hydrogen bonds as ice. Finally, there are reliable experimental indications that oxygen atoms in water confined in nanochannels are noticeably more ordered than in the bulk water; i.e., it is more similar to ice than to the bulk water [54,55].

Thus, the water confined in nanochannels of polymer membranes can be described by the Jaccard theory, using modified parameters of concentrations and motilities of defects.

In the following we will use this model to interpret our results on electroconductivity and self-diffusion in polymer electrolytes.

6. Discussion

We will start from the results shown in Fig. 1. The higher diffusion coefficient of water in polymer membranes obtained by the extrusion method by a factor of 1.5 is due to a more ordered system of oriented elongated channels. The change in the activation energy near 240 K can be explained as follows: In a rough approximation, the water in cylindrical channels is separated into two types, the water near the walls of a channel and the water in a central part, far away from the walls. The properties of the wall water can be strongly different from the properties of the bulk water. The origin of this difference is similar to that between bulk ice and its quasi-liquid surface layer. We suggest that the wall water has the diffusional activation energy of about 0.40 eV. At the same time, the water in a central part of the channel is identical to the bulk water with the activation energy of diffusion of about 0.20 eV. The central part of the channel provides the main contribution to the NMR signal at high temperatures because of its higher amount of molecules. Consequently, the measured activation energy is similar to that of the bulk water. When cooling to ~240 K water in the central part begins to crystallize or rather transform to the vitreous state [46], which reduces its contribution to the NMR signal because of a shorter spin-spin relaxation time in comparison with the wall water and larger loss of NMR signal during unavoidable dead time of spectrometer. It is remarkable that the maximum supercooling temperature of water is close to 240 K [38,56–58]. Below 240 K, the NMR signal is determined by the surface water, which has an activation energy of diffusion of ~0.40 eV. The transition at 240 K is smooth for two reasons: The interface between the wall and the bulk water is smooth and the channel diameters are distributed, leading to a distribution of the freezing parts.

Let us consider the dependence of the diffusion coefficient on the water content, presented in Fig. 2. It is reasonable to assume that by filling the channels the water is condensed first on the channel walls. Consequently, at a low water content the channels are filled incompletely and the contribution of water at the wall is larger. This explains the smaller diffusion coefficient at low water content. With increasing water content, the contribution of the bulk water rises, which leads to a higher diffusion coefficient measured by NMR. With decreasing temperature NMR measures again preferably the wall water. The mechanism of transition from bulk water diffusion at high temperatures to wall water diffusion at low temperatures is rather identical. The transition temperature is determined by crystallization of the bulk water; i.e., this

temperature should be approximately the same for both, the low and for the high water contents. In reality, since the amount of bulk water is smaller at low water content, the transition to the wall water regime should be slightly shifted toward higher temperatures, as can be seen in Fig. 2.

We now compare the results for proton diffusion with that for proton conductivity [44], presented in Fig. 3. At high water contents ($\lambda = 6.0$ and 6.6) diffusion and electroconductivity consistently show a transition at 240 K, with activation energy $E_a = 0.20$ eV above 240 K and 0.40 eV below. According to Ref. [58], the diffusion in bulk water is determined by bond defects and the activation energy of diffusion is close to the activation energy of migration of bond defects. At the same time, the low-frequency conductivity should be determined by minority carriers, which are usually ionic defects. The similarity of self-diffusion and conductivity seemingly contradicts [58]. However, in this case of Nafion, the number of ion defects generated by the protons from the acidic side chains of Nafion is so large that the partial conductivity of ionic defects becomes higher than the partial conductivity of bond defects; i.e., the ion defects become the majority carriers. Then, according to our model, the low-frequency conductivity is determined by bond defects. In fact, the water in nanochannels of polymer films is in a specific state, where the majority and minority carriers are interchanged as compared to pure bulk water. Such a phenomenon in physics of ice is known as crossover.

The transition between the high- and low-temperature regimes at low water contents ($\lambda = 2.0$ and 2.6) has specific features as compared to the transition at high water contents. The activation energies at high temperatures increases when reducing the water content at $\lambda \leq 2.6$. Such an increase can be attributed to a larger contribution of the wall water whose fraction at low water content is higher and the activation energy of diffusion in the wall water is higher. It is even possible that the number of water molecules at $\lambda \approx 2.0$ is so small that the wall water in fact constitutes a monolayer of adsorbed molecules with a higher activation energy. In addition, the carriers are different for diffusion and conductivity and the similarity between the temperature dependences of diffusion and conductivity is violated, as seen in Fig. 3.

The most interesting and surprising result of our analysis is that the majority carriers in water confined to nanochannels of Nafion films are the ion carriers, whereas the low-frequency conductivity is determined by bond defects. To confirm this conclusion, we present numerical estimates. The surface of the walls and the volume of the channel per unit length of the channels are $2\pi a$ and πa^2, respectively, where a is the radius of the channel. Consequently, the surface density of injected protons at which their number is equal to the number of bond defects (per unit length) is $\eta \approx an_B/2$. We estimate the defect density at 240 K as $n_B \approx 1.3 \times 10^{27}\ m^{-3}$ and $a = 2$ nm for the channel radius. Then, the surface density can be estimated as $\eta \approx 1.3 nm^{-2}$. This value corresponds to almost half of the surface density of the sulfite groups $\approx 78/32 \approx 2.44\ nm^{-2}$ [59]. This means that when half of the sulfite groups release their protons to water, the resulting concentration of the H_3O^+ defects becomes equal to that of the L defects. In reality, the ion defects will become majority carriers even at lower concentration because their mobility is higher than that of bond defects.

In summary, it can be concluded that a change in the type of the majority and minority carriers in channels of polymer membranes should take place, as confirmed by the similarity of Arrhenius plots for the self-diffusion coefficient and the conductivity.

7. Conclusions

We can summarize the main results of this study as follows:

The water in nanochannels of proton-exchange perfluorosulfonated membranes can be considered as existing in two states, wall water and central or bulk water. The water in these states can be characterized by different activation energies of diffusion and conductivity.

A smooth transition between the high and the low temperature diffusion regimes occurs at 240 K and is due to crystallization of the central water.

At low water content, $\lambda \leq 3$ the water molecules are preferably located in the vicinity of the wall and its activation energy is high. The proton injection from acid branches of side chains is so high that the ion defects become the majority carriers. The low-frequency conductivity is determined by the bond defects which are the majority carriers for this method.

In order to increase the proton transport, it is necessary to increase the concentration of the bond defects, which can be ensured by additional doping of the polymer matrix in a way that the dopant is induced into the channels. If this dopant will be able to orient the water molecules with their protons towards the dopant particles, an increase of the most mobile L-type bond defects occurs, thus increasing the low-temperature proton conductivity.

Declaration of competing interest

We have no conflict of interest declare.

CRediT authorship contribution statement

Elena Galitskaya: Writing - original draft, Data curation, Investigation, Methodology, Visualization, Conceptualization, Funding acquisition. **Alexei F. Privalov:** Writing - original draft, Methodology, Software. **Max Weigler:** Investigation, Methodology. **Michael Vogel:** Writing - original draft, Supervision, Writing - review & editing, Resources. **Alexei Kashin:** Formal analysis. **Mikhail Ryzhkin:** Formal analysis. **Vitaly Sinitsyn:** Writing - original draft, Conceptualization, Supervision, Validation, Writing - review & editing, Funding acquisition.

Acknowledgment

The work was supported by the Russian Science Foundation (project # 17-79-30054).

Appendix A. Supplementary data

Supplementary data to this article can be found online at https://doi.org/10.1016/j.memsci.2019.117691.

References

[1] Viral Mehta Joyce, Smith Cooper "Review and analysis of PEM fuel cell design and manufacturing", J. Power Sources 114 (2003) 132–153.
[2] W. Vielstich, A. Lamm, H.A. Gasteiger, Handbook of Fuel Cells, vols. 1–4, Wiley, Chichester, England, 2003.
[3] K.A. Mauritz, R.B. Moore, State of understanding of nafion, Chem. Rev. 104 (2004) 4535–4586.
[4] H.A. Gasteiger, W. Vielstich, H. Yokokawa, Handbook of Fuel Cells, vols. 5–6, John Wiley & Sons Ltd, Chichester, England, 2009.
[5] T.A. Zawodzinski Jr., C. Derouin, S. Radzinski, R.J. Sherman, V.T. Smith, T. E. Springer, S. Gottesfeld, Water uptake by and transport through Nafion® 117 membranes, J. Electrochem. Soc. 140 (1993) 1041–1047.
[6] Xiaobing Zhu, Huamin Zhang, Yu Zhang, Yongmin Liang, Xiaoli Wang, Baolian Yi, An ultrathin self-humidifying membrane for PEM fuel cell application: fabrication, characterization, and experimental analysis, J. Phys. Chem. B 110 (2006) 14240–14248.
[7] Thomas A. Zawodzinski Jr., Michal Neeman, Laurel O. Sillerud, Shimshon Cottesfeld, Determination of water diffusion coefficients in perfluorosulfonate ionomeric membranes, J. Phys. Chem. 95 (1991) 6040–6044.
[8] Klaus-Dieter Kreuer, Thomas Dippel, Wolfgang Meyer, Joachim Maier, NAFION@ membranes: molecular diffusion, proton conductivity and proton conduction mechanism, Mater. Res. Soc. Symp. Proc. 293 (1993) 273–282.
[9] Morihiro Saito, Naoko Arimura, Kikuko Hayamizu, Tatsuhiro Okada, Mechanisms of ion and water transport in perfluorosulfonated ionomer membranes for fuel cells, J. Phys. Chem. B 108 (2004) 16064–16070.
[10] Morihiro Saito, Kikuko Hayamizu, Tatsuhiro Okada, Temperature dependence of ion and water transport in perfluorinated ionomer membranes for fuel cells, J. Phys. Chem. B 109 (2005) 3112–3119.

[11] Pyoungho Choi, H. Nikhil, Jalani, Ravindra Datta, Thermodynamics and proton transport in nafion II. Proton diffusion mechanisms and conductivity, J. Electrochem. Soc. 152 (2005) E123–E130.
[12] Armel Guillermo, Gérard Gebel, Hakima Mendil-Jakani, Eric Pinton, NMR and pulsed field gradient NMR approach of water sorption properties in nafion at low temperature, J. Phys. Chem. B 113 (2009) 6710–6717.
[13] Zhao Qiao, Majsztrik Paul, Jay Benziger, Diffusion and interfacial transport of water in nafion, J. Phys. Chem. B 115 (2011) 2717–2727.
[14] Feina Xu, Sebastien Leclerc, Lottin Olivier, Daniel Canet, Impact of chemical treatments on the behavior of water in Nafion NRE-212 by ^{1}H NMR: self-diffusion measurements and proton quantization, J. Membr. Sci. 371 (2011) 148–154.
[15] Mathieu Klein, Jean-Christophe Perrin, Sebastien Leclerc, Laouès Guendouz, Jerome Dillet, Lottin Olivier, Anisotropy of water self-diffusion in a nafion membrane under traction, Macromolecules 46 (2013) 9259–9269.
[16] J. Li, K.G. Wilmsmeyer, L.A. Madsen, Anisotropic diffusion and morphology in perfluorosulfonate ionomers investigated by NMR, Macromolecules 42 (2009) 255–262.
[17] Mylene Robert, Assma El Kaddouri, Jean-Christophe Perrin, Sebastien Leclerc, Lottin Olivier, Towards a NMR-based method for characterizing the degradation of nafion XL membranes for PEMFC, J. Electrochem. Soc. 165 (6) (2018) F3209–F3216.
[18] Z. Ma, R. Jiang, M.E. Myers, E.L. Thompson, C.S. Gittleman, NMR studies of proton transport in fuel cell membranes at sub-freezing conditions, J. Mater. Chem. 21 (2011) 9302.
[19] K. Schmidt-Rohr, Q. Chen, "Parallel cylindrical water nanochannels in Nafion fuel-cell membranes", Nat. Mater. 7 (2008) 75–83.
[20] Klaus-Dieter Kreuer, Giuseppe Portale, A critical revision of the nano-morphology of proton conducting ionomers and polyelectrolytes for fuel cell applications, Adv. Funct. Mater. 23 (2013) 5390–5397.
[21] M.I. Ryzhkin, I.A. Ryzhkin, A.M. Kashin, E.A. Galitskaya, V.V. Sinitsyn, Proton conductivity in mesiporous materials, JETP Lett. (Engl. Transl.) 108 (2018) 596–600.
[22] M. Laporta, M. Pegoraro, L. Zanderighi, Perfluorosulfonated membrane (Nafion): FT-IR study of the state of water with increasing humidity, Phys. Chem. Chem. Phys. 1 (1999) 4619–4628.
[23] S.J. Paddison, Proton conduction mechanisms at low degrees of hydration in sulfonic acid –based polymer electrolyte membranes, Annu. Rev. Mater. Res. 33 (2003) 289–319.
[24] Georgios Polizos, Zijie Lu, Digby D. Macdonald, Evangelos Manias, State of water in nafion 117 proton exchange membranes studied by dielectric relaxation spectroscopy, Mater. Res. Soc. Symp. Proc. 972 (2007) AA08–11.
[25] Zijie Lu, Georgios Polizos, Digby D. Macdonald, E. Mania, State of water in perfluorosulfonic ionomer (nafion 117) proton exchange membranes, J. Electrochem. Soc. 155 (2) (2008) B163–B171.
[26] V.F. Petrenko, R.W. Whitworth, Physics of Ice, Oxford Univ. Press, New York, 1999.
[27] D. Demuth, M. Sattig, E. Steinrucken, M. Weigler, M. Vogel, 2H NMR studies on the dynamics of pure and mixed hydrogen-bonded liquids in confinement, Z. Phys. Chem. 232 (7–8) (2018) 1059–1087.
[28] M. Rosenstihl, K. Kämpf, F. Klameth, M. Sattig, M. Vogel, Dynamics of interfacial water, J. Non-Cryst. Sol. 407 (2015) 449–458.
[29] M. Sattig, S. Reutter, F. Fujara, M. Werner, G. Buntkowsky, M. Vogel, NMR studies on the temperature-dependent dynamics of confined water, Phys. Chem. Chem. Phys. 16 (2014) 19229–19240.
[30] M. Vogel, NMR studies on simple liquids in confinement, Eur. Phys. J. Spec. Top. 189 (2010) 47–64.
[31] M. Weigler, M. Brodrecht, G. Buntkowsky, M. Vogel, Reorientation of deeply cooled water in mesoporous silica: NMR studies of the pore-size dependence, J. Phys. Chem. B 123 (2019) 2123–2134.
[32] I. Chang, F. Fujara, B. Geil, G. Hinze, H. Sillescu, A. Tölle, New perspectives of NMR in ultrahigh static magnetic field gradients, J. Non-Cryst. Solid 172–174 (1994) 674.
[33] William S. Price, Pulsed-field gradient nuclear magnetic resonance as a tool for studying translational diffusion: Part 1. basic theory, Concepts Magn. Reson. 9 (5) (1997) 299–336.
[34] V.V. Sinitsyn, A.I. Privalov, O. Lips, A.I. Baranov, D. Kruk, F. Fujara, Transport properties of $CsHSO_4$ investigated by impedance spectroscopy and nuclear magnetic resonance, Ionics 14 (2008) 223–226.
[35] G. Fleischer, F. Fujara, NMR as a generalized incoherent scattering experiment, in: B. Blümich (Ed.), Solid-State NMR I Methods. NMR, Basic Princ. Progress, vol. 30, 1994, pp. 159–207.
[36] B. MacMillan, A. Sharp, R. Armstrong, An n.m.r. investigation of the dynamical characteristics of water absorbed in Nafion, Polymer 40 (1999) 2471–2480.
[37] C.J. Van Oss, in: F. Franks (Ed.), A Review of: "Water a Comprehensive Treatise Volume 7 (Water and Aqueous Solutions at Subzero Temperatures, Plenum Press, New York, 1982.
[38] R.J. Speedy, C.A. Angell, Isothermal compressibility of supercooled water and evidence for a thermodynamic singularity at −45°C, J. Chem. Phys. 65 (1976) 851–858.
[39] S.P. Rowland (Ed.), Water in Polymers, American Chemical Society, Washington, D. C., 1980.
[40] A. Stassi, I. Gatto, E. Passalacqua, V. Antonucci, A.S. Arico, L. Merlo, C. Oldani, E. Pagano, Performance comparison of long and short-side chain perfluorosulfonic membranes for high temperature polymer electrolyte membrane fuel cell operation, J. Power Sources 196 (2011) 8925–8930.
[41] A.S. Aricò, A. Di Blasi, G. Brunaccini, F. Sergi, G. Dispenza, L. Andaloro, M. Ferraro, V. Antonucci, P. Asher, S. Buche, D. Fongalland, G.A. Hards, J.D.B. Sharman, A. Bayer, G. Heinz, N. Zandonà, R. Zuber, M. Gebert, M. Corasaniti, A. Ghielmi, D. J. Jones, High temperature operation of a solid polymer electrolyte fuel cell stack based on a new ionomer membrane, Fuel Cells 10 (2010) 1013–1023.
[42] T.E. Springer, T.A. Zawodinski, S. Gottesfeld, Polymer electrolyte fuel cell model, J. Electrochem. Soc. 138 (1991) 2334–2341.
[43] Y. Wang, P.P. Mukherjee, J. Mishler, R. Mukundan, R.L. Borup, Cold start of polymer electrolyte fuel cells: three-stage startup characterization, Electrochim. Acta 55 (2010) 2636–2644.
[44] E.L. Thompson, T.W. Capehart, Timothy J. Fuller, Jorne Jacob, Investigation of low-temperature proton transport in nafion using direct current conductivity and differential scanning calorimetry, J. Electrochem. Soc. 153 (2006) A2351–A2362.
[45] V.G. Artemov, I.A. Ryzhkin, V.V. Sinitsyn, Similarity of the dielectric relaxation processes and transport characteristics in water and ice, JETP Lett. (Engl. Transl.) 102 (2015) 41–45.
[46] A. Kusoglu, A.Z. Weber, New insights into perfluorinated sulfonic-acid ionomers, Chem. Rev. 117 (2017) 987–1104.
[47] C. Jaccard, Thermodynamics of irreversible processes applied to ice", Phys. Kondens. Mater. 3 (1964) 99–118.
[48] M. Hubmann, Polarization processes in the ice lattice, Z. Phys. B 32 (1979) 127.
[49] A.V. Klyuev, I.A. Ryzhkin, M.I. Ryzhkin, Generalized dielectric permittivity of ice, JETP Lett. (Engl. Transl.) 100 (2014) 604–608.
[50] A.I. Ryzhkin, M.I. Ryzhkin, A.M. Kashin, E.A. Galitskaya, V.V. Sinitsyn, High proton conductivity state of water in nanoporous materials, Europhys. Lett. 126 (2019) 36003–36010.
[51] M.I. Ryzhkin, A.V. Klyuev, V.V. Sinitsyn, I.A. Ryzhkin, Liquid state of hydrogen bond, JETP Lett. 104 (2016) 248–252.
[52] M.I. Ryzhkin, I.A. Ryzhkin, V.V. Sinitsyn, A.V. Klyuev, Model of a surface liquid-like layer of ice, JETP Lett. 106 (2017) 760–764.
[53] I.A. Ryzhkin, R.W. Whitworth, The configurational entropy in the Jaccard theory of the electrical properties of ice, J. Phys. Condens. Matter 9 (1997) 395–401.
[54] F. Corsetti, O. Matthews, E. Artacho, Structural and configurational properties of nanoconfined monolayer ice from first principles, Sci. Rep. 6 (2016) 18651. https://www.nature.com/articles/srep18651.
[55] S. Strazdaite, J. Versluis, E.H.G. Backus, H.J. Bakker, Enhanced ordering of water at hydrophobic surfaces, J. Chem. Phys. 140 (2014) 054701–054711.
[56] C.A. Angell, in: F. Franks (Ed.), Water: A Comprehensive Treatise, vol. 7, 1972. Plenum, New York.
[57] H. Kanno, C.A. Angell, Water: anomalous compressibilities to 1.9 kbar and correlation with supercooling limits, J. Chem. Phys. 70 (1979) 4008–4016.
[58] Lars Onsager, L.K. Runnels, Diffusion and relaxation phenomena in ice, J. Chem. Phys. 50 (1969) 1089–1103.
[59] Pyoungho Choi, H. Nikhil, Jalani, Ravindra Datta, Thermodynamics and proton transport in nafion II. Proton diffusion mechanisms and conductivity, J. Electrochem. Soc. 152 (3) (2005) E123–E130.